Robust Delay-Dependent Load Frequency Control of Wind Power System Based on a Novel Reconstructed Model

Li Jin, *Student Member, IEEE,* Yong He, *Senior Member, IEEE,* Chuan-Ke Zhang, *Member, IEEE,* Xing-Chen Shangguan, *Student Member, IEEE,* Lin Jiang, *Member, IEEE,* and Min Wu, *Fellow, IEEE*

***Abstract*—This paper presents a novel reconstructed model for the delayed load frequency control (LFC) schemes considering wind power, which aims to improve the computational efficiency for PID controllers while retaining their dynamic performance. Via fully exploiting system states influenced by time delays directly, this novel reconstructed method is proposed with controller isolated. Hence, when the PID controllers are unknown, the stability criterion based on this model can resolve controller gains with less time consumed. For given PID gains, this model can be employed to establish criteria for stability analysis which can realize the tradeoff between the calculation accuracy and efficiency. Case study is firstly based on a two-area traditional LFC system to validate the merits of novel reconstructed model, including accurately estimating the influence of time delay on system frequency stability with increased computation capability. Then, under traditional and deregulated environments, case studies are carried out on the two-area and three-area schemes, respectively. Through the novel reconstructed model, the efficiency of obtaining controller parameters is highly improved while their robustness against the random wind power, tie-line power changes, inertial reductions, and time delays remains almost unchanged.**

***Index Terms*—Load frequency control, communication delays, model reconstruction, stability analysis, controller design**

I. Introduction

Load frequency control (LFC) has been employed by the power system such that its frequency and power interchanges can be maintained at scheduled values [1]. The traditional LFC system utilizes dedicated communication channels to transmit control signal and measurement data [2]. Under deregulated environment, these communication channels are employed to support the bilateral protocol between generation companies (Gencos) and distribution companies (Discos). Such networks introduce time delays, which affects the stability of system frequency [3], [4]. Also, the injection of wind power into power system solves two problems, i.e., the poor storage of non-renewable energy resources and the seriously environmental pollution arisen from consuming fossil energy [5]. The wind power has features of intermittency and fluctuations and its high penetration also makes challenges to power system in maintaining the frequency balance since replacing the conventional generators with wind turbines leads to low or zero inertia [6]. The main grid does not have sufficient regulation capability to maintain system frequency deviation within a specified range [7]. Therefore, it is necessary to investigate the influences that both time delay and wind power have on the frequency stability in the LFC schemes such that the robust control strategy can be designed to eliminate these kinds of impacts.

Since the actual time delay is stochastic and time-varying, current researches tend to use time domain method including Lyapunov-Krasovskii method to derive linear matrix inequalities (LMIs) such that the maximum allowable delay upper bound called delay margin can be calculated [8]. For delayed LFC schemes, via constructing appropriate Lyapunov-Krasovskii functional (LKF) and bounding its derivative with conservatism-reduced inequalities, the improved delay-dependent stability conditions are derived in terms of LMIs [9], [10] to obtain the delay margins with increased accuracy. In fact, the model of power system is naturally high-dimension. The derived LMIs that based on the original model have difficulty in determining delay margin with computation efficiency, especially for the multi-area LFC schemes. Via considering the sparsity of the LFC model, [11] tends to reduce the maximal order of LMIs to speed up the calculation. A transform matrix is defined such that all system states in the original model can be decomposed into the delayed part and the delay-irrelated part, and the LKF is constructed using the low-order delayed part [12]. When the system is equipped with the PID controller, this division is too strict to be realized. Hence, by introducing a new composition method, a reconstructed method is proposed [13], based on which the stability criterion

This work is supported by the National Natural Science Foundation of China under Grants 61973284, 62022074, and 61873347, the Hubei Provincial Natural Science Foundation of China under Grants 2019CFA040, the 111 Project under Grant B17040, the Fundamental Research Funds for National Universities, China University of Geosciences (Wuhan), and the Program of China Scholarship Council under Grants 201706410037 and 201706410012. (*Corresponding author: Yong He.*)

L. Jin, and X.C. Shangguan are with the School of Automation, China University of Geosciences, Wuhan, 430074, China, and with Hubei Key Laboratory of Advanced Control and Intelligent Automation for Complex Systems, Wuhan, 430074, China, and with Engineering Research Center of Intelligent Technology for Geo-Exploration, Ministry of Education, Wuhan, 430074, China, and also with the Department of Electrical Engineering and Electronics, University of Liverpool, Liverpool L69 3GJ, United Kingdom. (Email: jinli@cug.edu.cn; star@cug.edu.cn).

Y. He, C.K. Zhang, and M. Wu are with the School of Automation, China University of Geosciences, Wuhan, 430074, China, and with Hubei Key Laboratory of Advanced Control and Intelligent Automation for Complex Systems, Wuhan, 430074, China, and also with Engineering Research Center of Intelligent Technology for Geo-Exploration, Ministry of Education, Wuhan, 430074, China. (Email: heyong08@cug.edu.cn; ckzhang@cug.edu.cn; wumin@cug.edu.cn).

L. Jiang is with the Department of Electrical Engineering and Electronics, University of Liverpool, Liverpool L69 3GJ, United Kingdom. (Email: ljiang@liverpool.ac.uk).

is established to obtain delay margins with highly improved computation accuracy and efficiency. Whereas, the selection of a transformation matrix relies on finding non-zero elements in the coefficient matrix of the delayed state. In some cases, we find the calculation accuracy is decreased a lot through using the reconstructed model in comparison with the original model. There lacks a novel method to reconstruct model standing on the special features of delayed power system so that a tradeoff between the computation accuracy and efficiency is achieved.

In order to reduce the influence that time delays have on the system dynamics, some research works are presented, i.e., the robust LFC strategies are presented based on the H_∞ theory [14], [15]. Focusing on the problems caused by introducing wind power into power system, some researches aim to determine the highest penetration level that guarantees the stable operation of the system [16]. The virtual synchronous machine (VSM) was developed to compensate the inertia reduction when the parameters of VSM are appropriately adjusted [17]. Note that these parameters cannot be guaranteed to be applicable in the practical synchronous generators. Hence, by introducing an index of decay rate related to settling time [18], the exponential stability of the delayed power system is analyzed using Lyapunov-Krasovskii method and therefore, the decay rate-based state feedback controller is designed, which have robustness against the inertia reduction [19]. As we all known, not all system states can be detected conveniently and the PID-type LFC controllers are alternative. Note that all of these controller gains are obtained based on the original model. When the multi-area LFC schemes are considered, it is complex and time consumed that the improved cone complementarity linearization (ICCL) algorithm is employed to obtain the optimal parameters for PID controller [14]. A reconstructed approach was presented in [13], based on which the stability analysis of delayed LFC scheme is realized with enhanced accuracy and calculation efficiency. Despite that, since this method relies on the value of PID gains, the derived criterion is unable to guide the design of controllers. Therefore, a novel reconstructed method needs to be investigated such that it enables controller parameters to be calculated efficiently.

This paper focuses on proposing a novel reconstructed approach for the LFC scheme with time delay and wind power, which enables to compute controller gains. Moreover, both increased efficiency and dynamic performance are guaranteed. When compared the method presented in [13], the method proposed in this paper further increase the calculation accuracy with the little cost of computation efficiency. Firstly, via considering the states that are directly influenced by the time delay in the input channel, a proper transfer matrix is exploited to develop a novel reconstructed model. Secondly, this novel reconstructed method is able to separate the gain matrix apart from the input and output matrix. Based on the Lyapunov theory and the novel reconstructed model, the asymptotical stability criterion is established at first in terms of LMIs. These LMIs are able to derive accurate delay margins with increased efficiency. To address the aforementioned problems coming from wind power, the asymptotical condition is extended to provide the constraint between time delay and the index of decay rate such that the exponential stability of power system can be guaranteed. This exponential criterion is capable of guiding the development of decay rate-based PID controllers with high efficiency. In addition, the robustness of these controllers against wind power disturbance, tie line power changes, inertia reduction, and time delays is expected to be unchanged in comparison with that based on the original model.

The remainder of this paper is organized as follows. Section II shows the original model of the multi-area LFC schemes whose reconstructed formes are realized by proposing a novel approach. Section III provides asymptotical stability conditions considering both the models before and after reconstructed and then, extends them to exponentially stable criteria. In Section IV, case studies are carried out on the two-area and three-area LFC schemes under the traditional and deregulated environments, respectively to validate the effectiveness of proposed novel reconstructed model. Finally, Section V comes to the conclusions.

II. Dynamic Models of multi-area LFC schemes

This section models the LFC power system with time delay and wind power at first. Then, a novel method is investigated to turn the original system model into the reconstructed one. The stability conditions established based on this reconstructed model can provide guidance for obtaining controller gains with increased efficiency while guaranteeing their dynamic performance.

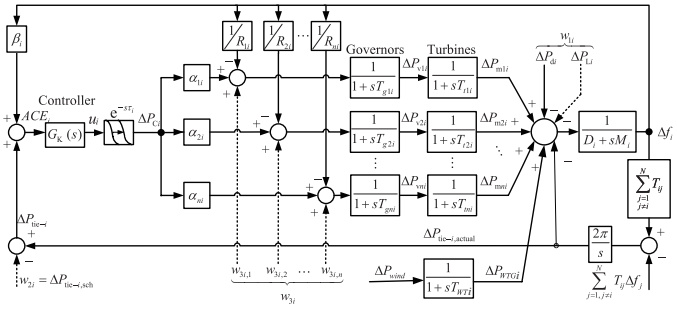

Fig. 1. Configuration of control area i (Traditional LFC: without dotted line; Deregulated LFC: with dotted line).

A. Original model

Fig. 1 shows the structure of area i, in which n Gencos equipped with non-reheat turbines, m Discos, and a PID controller are involved. Exponential block $e^{-s\tau_i}$ represents the delays arising in the transmission channels. Other notations are mentioned in [13].

When the dotted line connections used in Fig. 1 are ignored, the model of area i in the multi-area traditional LFC scheme with N areas included is described as:

$$\begin{cases} \dot{x}_i(t) = A_i x_i(t) + B_i u_i(t-\tau_i) + F_i \omega_i \\ y_i(t) = C_i x_i(t) \end{cases} \tag{1}$$

where

$$x_i = [\Delta f_i, \Delta P_{tie-i}, \Delta P_{m1i}, \cdots, \Delta P_{mni}, \Delta P_{v1i}, \cdots, \Delta P_{vni}, \Delta P_{WTGi}]^T, y_i = ACE_i,\ \Delta P_{Ci} = u_i(t-\tau_i)$$

$$\omega_i^T = \left[\Delta P_{\mathrm{d}i},\ \sum_{j=1,j\neq i}^{N} T_{ij}\Delta f_j, \Delta P_{\mathrm{wind}}\right]$$

$$A_i = \begin{bmatrix} A_{11i} & A_{12i} & 0 & A_{14i} \\ 0 & A_{22i} & A_{23i} & 0 \\ A_{31i} & 0 & A_{33i} & 0 \\ 0 & 0 & 0 & -\frac{1}{T_{WTi}} \end{bmatrix}, B_i = \begin{bmatrix} 0 \\ 0 \\ B_{3i} \\ 0 \end{bmatrix}$$

$$A_{11i} = \begin{bmatrix} -\frac{D_i}{M_i} & -\frac{1}{M_i} \\ 2\pi\sum_{j=1,j\neq i}^{N} T_{ij} & 0 \end{bmatrix}, A_{12i} = \begin{bmatrix} \frac{1}{M_i} & \cdots & \frac{1}{M_i} \\ 0 & \cdots & 0 \end{bmatrix}$$

$$A_{14i} = \begin{bmatrix} \frac{1}{M_i} \\ 0 \end{bmatrix}, A_{22i} = -A_{23i} = -\mathrm{diag}\left\{\frac{1}{T_{t1i}}, \cdots, \frac{1}{T_{tni}}\right\}$$

$$A_{31i} = -\begin{bmatrix} \frac{1}{R_{1i}T_{t1i}} & \cdots & \frac{1}{R_{ni}T_{tni}} \\ 0 & \cdots & 0 \end{bmatrix}^T, B_{3i} = \left[\frac{\alpha_{1i}}{T_{g1i}}, \cdots, \frac{\alpha_{ni}}{T_{gni}}\right]^T$$

$$A_{33i} = -\mathrm{diag}\left\{\frac{1}{T_{g1i}}, \cdots, \frac{1}{T_{gni}}\right\}, C_i = [\beta_i, 1, 0]$$

$$F_i = \begin{bmatrix} -\frac{1}{M_i} & 0 & 0 \\ 0 & -2\pi & 0 \\ 0 & 0 & 0 \\ 0 & 0 & \frac{1}{T_{WTi}} \end{bmatrix}$$

with ΔP_{WTGi} and T_{WTi} being wind turbine generator output power change and wind turbine generator time constants respectively, and other notations are defined in [13].

In Fig. 1, when the dotted line connections that represent the new load demands based on the deregulated contract are taken into account, we can obtain the following model for area i contained in the multi-area deregulated LFC scheme with N areas.

$$\begin{cases} \dot{x}_i(t) = A_i x_i(t) + B_i u_i(t-\tau_i) + F_i\omega_i \\ y_i(t) = C_i x_i(t) \end{cases} \tag{2}$$

where A_i, B_i and C_i are defined identically to equation (3), and notations ω_i and F_i are redefined as

$$\omega_i^T = \left[\mathrm{w}_{1i},\ \sum_{j=1,j\neq i}^{N} T_{ij}\Delta f_j, \mathrm{w}_{2i}, \mathrm{w}_{3i}, \Delta P_{\mathrm{wind}}\right]$$

$$F_i = \begin{bmatrix} F_{1i} & 0 & 0 \\ 0 & 0 & 0 \\ 0 & F_{2i} & 0 \\ 0 & 0 & \frac{1}{T_{WTi}} \end{bmatrix}, F_{1i} = \begin{bmatrix} -\frac{1}{M_i} & 0 & 0 \\ 0 & -2\pi & -1 \end{bmatrix}$$

$$F_{2i} = \mathrm{diag}\left\{\frac{1}{T_{g1i}}, \cdots, \frac{1}{T_{gni}}\right\}$$

The construction of a multi-area LFC scheme is formed by connecting area to area, and the interactions or coupling terms between different regions are regarded as disturbances. Compared with the traditional LFC scheme, in the deregulated LFC scheme, the new demand signals can be seen as additional disturbances. Moreover, due to analyzing the internal stability of system, the external disturbances can be ignored and the following model is capable of describing both the power systems under traditional and deregulated environments.

$$\begin{cases} \dot{x}_i(t) = A_i x_i(t) + B_i u_i(t-\tau_i) \\ y_i(t) = C_i x_i(t) \end{cases} \tag{3}$$

The PID-type LFC controller in area i is designed as

$$u_i(t) = K_{Pi}ACE_i + K_{Ii}\int ACE_i dt + K_{Di}\frac{d}{dt}ACE_i.$$

When defining two virtual vectors $\bar{x}_i = [x_i^T \ \int y_i^T dt]^T$ and $\bar{y}_i = [y_i^T \ \int y_i^T dt \ (d/dt)y_i^T]^T$, we can develop the closed-loop model for the delayed LFC scheme as follow.

$$\begin{cases} \dot{\bar{x}}_i(t) = \bar{A}_i\bar{x}_i(t) + \bar{B}_i K_i \bar{C}_i \bar{x}_i(t-\tau_i) \\ \bar{y}_i(t) = \bar{C}_i\bar{x}_i(t) \end{cases} \tag{4}$$

where

$$\bar{A}_i = \begin{bmatrix} A_i & 0 \\ C_i & 0 \end{bmatrix}, \bar{B}_i = \begin{bmatrix} B_i \\ 0 \end{bmatrix}, \bar{C}_i = \begin{bmatrix} C_i & 0 \\ 0 & 1 \\ C_iA_i & 0 \end{bmatrix}, K_i = [K_{Pi}K_{Ii}K_{Di}].$$

B. Novel reconstructed model

The stability criteria established directly based on the whole system model (4) are reported to have computational difficulties in checking the LMI-based conditions and determining delay margins. The latest literature tends to propose a composition method to reconstruct the system model with a delayed part and a delay-free part [13]. The construction of the LKF candidate is mainly based on the lower-order delayed part in order to decrease the order of the LMI-based criteria while increasing its computational performance. However, this composition method highly depends on finding elements that are not-zero from the coefficient matrices, but the special features of the delayed LFC scheme are not concerned. As a result, it is hard to realize a tradeoff between the computation accuracy and efficiency based on the model presented in [13]. Moreover, the value of coefficient matrices plays a significant role in determining the composition method, which will be ineffective if the controller gains remain designed. That is, the existing reconstructed method is unable to be used for designing controller gains. Thus, a novel reconstructed model needs to be proposed in this paper by analyzing the special features of system (4) based on the diagram of Fig.1.

Fig. 1 reveals that, in area i, time delays are introduced into the control input channel through

$$\Delta P_{Ci}(t) = u_i(t-\tau_i) \tag{5}$$

which directly affects states $\Delta P_{vki}(t)$. The relationship can be expressed with

$$\Delta\dot{P}_{vki}(t) = f(\Delta f_i(t), \Delta P_{vki}(t)) + \frac{\alpha_{ki}}{T_{gki}}u_i(t-\tau_i)$$

where $f(\cdot)$ is an appropriate function.

Define $\bar{x}_{i2} = [\Delta P_{v1i}(t), \cdots, \Delta P_{vni}(t)]^T \in R^{n_2}$ and $\bar{x}_{i1} = \bar{x}_i - \bar{x}_{i2} \in R^{n_1}$. Hence, by pre-multiplying with a

suitable transfer matrix T_1, we can obtain $T_1\bar{x}_i(t)=\begin{bmatrix}\bar{x}_{i1}\\ \bar{x}_{i2}\end{bmatrix}$, and therefore, system (4) can be turned into

$$\begin{bmatrix}\dot{\bar{x}}_{i1}\\ \dot{\bar{x}}_{i2}\end{bmatrix}=T_1\bar{A}_iT_1^{-1}\begin{bmatrix}\bar{x}_{i1}\\ \bar{x}_{i2}\end{bmatrix}+T_1\bar{B}_iK_i\bar{C}_iT_1^{-1}\begin{bmatrix}\bar{x}_{i1}(t-\tau_i)\\ \bar{x}_{i2}(t-\tau_i)\end{bmatrix}.$$

Its equivalent form is

$$\begin{cases}\dot{\bar{x}}_{i1}(t)=A_{i11}\bar{x}_{i1}(t)+A_{i12}\bar{x}_{i2}(t)\\ \dot{\bar{x}}_{i2}(t)=A_{i21}\bar{x}_{i1}(t)+A_{i22}\bar{x}_{i2}(t)+b_iK_ic_i\bar{x}_{i1}(t-\tau_i)\end{cases}\tag{6}$$

where

$$T_1\bar{A}_iT_1^{-1}=\begin{bmatrix}A_{i11} & A_{i12}\\ A_{i21} & A_{i22}\end{bmatrix},T_1\bar{B}_i=\begin{bmatrix}0\\ b_i\end{bmatrix},\bar{C}_iT_1^{-1}=[c_i,0].$$

Since the row number of states $\Delta P_{vki}(t), i=1,2,\cdots,n$ ranges from $3+n$ to $2+2n$ in state vector x, in order to separate them from the whole state vector, we can define nonsingular matrix T_1 as

$$T=[E_1,E_2,\cdots,E_{2+n},E_{3+2n},E_{4+2n},E_{3+n},\cdots,E_{2+2n}]^T\tag{7}$$

where $E_k=[0_{1\times(k-1)},1,0_{1\times(2n+3-k)}]^T$.

Considering equation (7), transfer matrix T_1 can be determined by the locations of states $\Delta P_{vki}(t), i=1,2,\cdots,n$, i.e., if the number of generators is given, the order of system model (4) will be determined to obtain T_1 intuitively. Unlike this paper, the method in [13] focuses on finding the non-zero elements in matrix $B_iK_iC_i$ through using mathematical analysis in order to find transfer matrix T_1. Due to the ignorance of the special physical characteristics of the delayed LFC scheme, the existing method can realize increased computation efficiency, but the conservatism introduced by using the existing method for analyzing delay-dependent stability still remains to be further reduced.

In addition, to investigate the delay-dependent stability analysis of the LFC scheme involving time delays, based on the time domain method, we need to construct an LKF candidate making use of information on the length of time delays. In this way, the conservatism of delay-dependent conditions is reduced, and they are expected to derive allowable maximum delay margins. Hence, in Section III, considering the original model (4), the time delays are contained in $\bar{x}_i\in R^{n_1+n_2}$ which is required to construct the LKF. Whereas, the reconstructed model (6) only contains the information of time delays in state $\bar{x}_{i1}\in R^{n_1}$ whose order is far less than $\bar{x}_i$. Thus, Section IV will show that the construction of the LKF mainly based on $\bar{x}_{i1}$ does not introduce increased conservatism into the delay-dependent conditions developed, but their computational efficiency is greatly improved.

Most importantly, the novel reconstructed model (6) is available for obtaining controller gains using the Lyapunov theory. Controller gain K_i is always segmented apart from input matrix $\bar{B}_i$ and output matrix $\bar{C}_i$. By contrast, the approach presented in [13] is applied to a system model with totally known coefficient matrices, and the choice of transfer matrix T_1 highly depends on the value of gain K_i. Hence, this method can only be used for investigating the stability of delayed power systems. If the controller gains remain to be resolved, the method in [13] will be infeasible. In Section IV, it will be validated that, based on the Lyapunov theory, the proposed model enables to design controller gains with greatly improved efficiency while guaranteeing the dynamic performance of obtained controllers.

III. Delay dependent stability analysis

Based on the Lyapunov theory, this section provides two stability conditions. Firstly, the delay-dependent asymptotically stable condition is derived based on the novel reconstructed model, which can be used to achieve almost accurate delay upper bounds with increased efficiency in comparison with that relying on the original model. Secondly, the asymptotically stable condition is extended to the condition of exponential stability for the delayed power system with wind power integrated. It can be used to optimize decay rate-based PID controllers by minimizing the decay rate α with the PSO algorithm for a preset delay upper bound. The time spent on calculating PID gains is reduced through using the criterion based on the novel reconstructed model while the dynamic performance of designed controller is also guaranteed.

A. Asymptotical stability criterion

This part presents an asymptotical stability condition for the delayed power system considering wind power. In order to show the utilization of novel reconstructed model only introduces little conservatism, the started part of Theorem 1 is based on the original model, and its second part is dependent on the novel reconstructed model.

Theorem 1. *For given scalars τ_i, system (4) is asymptotical stable, if one of the following conditions holds*
C1: there exist symmetric $2n\times2n$ matrix $P_i>0$, symmetric $n\times n$ matrices $Q_i>0, R_i>0$, such that the following inequality holds

$$\Pi_i<0\tag{8}$$

where

$$\Pi_i=\begin{bmatrix}e_1\\ \tau_ie_3\end{bmatrix}^TP_i\begin{bmatrix}e_{si}\\ e_1-e_2\end{bmatrix}+\begin{bmatrix}e_{si}\\ e_1-e_2\end{bmatrix}^TP_i\begin{bmatrix}e_1\\ \tau_ie_3\end{bmatrix}+e_1^TQ_ie_1-e_2^TQ_ie_2+\tau_i^2e_{si}^TR_ie_{si}-\begin{bmatrix}e_1-e_2\\ e_1+e_2-2e_3\end{bmatrix}^T\begin{bmatrix}R_i & 0\\ 0 & 3R_i\end{bmatrix}\begin{bmatrix}e_1-e_2\\ e_1+e_2-2e_3\end{bmatrix}$$

$$e_{si}=\bar{A}_ie_1+\bar{B}_iK_i\bar{C}_ie_2$$

$$e_j=\left[0_{n\times(j-1)n},I_{n\times n},0_{n\times(3-j)n}\right],j=1,2,3.$$

C2: there exist symmetric $(2n_1+n_2)\times(2n_1+n_2)$ matrix $U_i>0$, symmetric $n_1\times n_1$ matrices $H_i>0,W_i>0$, such that the following inequality holds

$$\Theta_i<0\tag{9}$$

where

$$\Theta_i=\begin{bmatrix}\vartheta_1\\ \vartheta_0\\ \tau_i\vartheta_3\end{bmatrix}^T U_i\begin{bmatrix}\vartheta_{\iota i}\\ \vartheta_{\kappa i}\\ \vartheta_1-\vartheta_2\end{bmatrix}+\begin{bmatrix}\vartheta_{\iota i}\\ \vartheta_{\kappa i}\\ \vartheta_1-\vartheta_2\end{bmatrix}^T U_i\begin{bmatrix}\vartheta_1\\ \vartheta_0\\ \tau_i\vartheta_3\end{bmatrix}+\vartheta_1^T H_i\vartheta_1-\vartheta_2^T H_i\vartheta_2$$
$$+\tau_i^2\vartheta_{\iota i}^T W_i\vartheta_{\iota i}-\begin{bmatrix}\vartheta_1-\vartheta_2\\ \vartheta_1+\vartheta_2-2\vartheta_3\end{bmatrix}^T\begin{bmatrix}W_i & 0\\ 0 & 3W_i\end{bmatrix}\begin{bmatrix}\vartheta_1-\vartheta_2\\ \vartheta_1+\vartheta_2-2\vartheta_3\end{bmatrix}$$
$$\vartheta_{\iota i}=A_{i11}\vartheta_1+A_{i12}\vartheta_0$$
$$\vartheta_{\kappa i}=A_{i21}\vartheta_1+A_{i22}\vartheta_0+b_iK_ic_i\vartheta_2$$
$$\vartheta_j=\left[0_{n_1\times(j-1)n_1},I_{n_1\times n_1},0_{n_1\times(3-j)n_1},0_{n_1\times n_2}\right],j{=}1,2,3$$
$$\vartheta_0=\left[0_{n_2\times 3n_1},I_{n_2\times n_2}\right].$$

Proof. Considering the original model (4), the following general LKF used for analyzing the delay-dependent stability of delayed systems is recalled from [20].

$$V_i(t)=\begin{bmatrix}\bar{x}_i(t)\\ \int_{t-\tau_i}^t\bar{x}_i(s)ds\end{bmatrix}^T P_i\begin{bmatrix}\bar{x}_i(t)\\ \int_{t-\tau_i}^t\bar{x}_i(s)ds\end{bmatrix}+\int_{t-\tau_i}^t\bar{x}_i^T(s)Q_i\bar{x}_i(s)ds+\tau_i\int_{-\tau_i}^0\int_{t+\theta}^t\dot{\bar{x}}_i^T(s)R_i\dot{\bar{x}}_i(s)dsd\theta \tag{10}$$

where P_i, Q_i, R_i are symmetric positive-definite matrices.

The derivative of $V_i(t)$ is calculated along system (4). When employing the same procedure for analyzing delayed power system in [13], we can obtain

$$\dot{V}_i(t)\le\zeta_i^T(t)\Pi_i\zeta_i(t) \tag{11}$$

with $\zeta_i^T(t)=[\bar{x}_i^T(t),\bar{x}_i^T(t-\tau_i),\frac{1}{\tau_i}\int_{t-\tau_i}^t\bar{x}_i^T(s)ds]$. Hence, the holding of criterion in Theorem 1.C1 leads to $\dot{V}_i(t)\le-\varepsilon\|\bar{x}_i(t)\|^2$ with a sufficient small scalar $\varepsilon>0$, which guarantees the asymptotical stability for system (14).

Based on the reconstructed model (6), the time delay information is included in states $\bar{x}_{i1}(t)$. Hence, by replacing the terms that are used to deal with the delayed states in the LKF (10), we have the following newly constructed LKF.

$$\tilde{V}_i(t)=\begin{bmatrix}\bar{x}_{i1}(t)\\ \bar{x}_{i2}(t)\\ \int_{t-\tau_i}^t\bar{x}_{i1}(s)ds\end{bmatrix}^T U_i\begin{bmatrix}\bar{x}_{i1}(t)\\ \bar{x}_{i2}(t)\\ \int_{t-\tau_i}^t\bar{x}_{i1}(s)ds\end{bmatrix}+\int_{t-\tau_i}^t\bar{x}_{i1}^T(s)H_i\bar{x}_{i1}(s)ds+\tau_i\int_{-\tau_i}^0\int_{t+\theta}^t\dot{\bar{x}}_{i1}^T(s)W_i\dot{\bar{x}}_{i1}(s)dsd\theta \tag{12}$$

where U_i, H_i, and W_i are symmetric positive definite matrices.

Similarly, when the derivative of $\tilde{V}_i(t)$ is calculated along system (6), it is convenient to obtain

$$\dot{\tilde{V}}_i(t)\le\xi_i^T(t)\Theta_i\xi_i(t) \tag{13}$$

with $\xi_i^T(t)=[\bar{x}_{i1}^T(t),\bar{x}_{i1}^T(t-\tau_i),\frac{1}{\tau_i}\int_{t-\tau_i}^t\bar{x}_{i1}^T(s)ds,\bar{x}_{i2}^T(t)]$, and therefore, the asymptotical stability of system (6) is guaranteed.

As can be seen from the LKF (10), its augmented term and Q_i and R_i-dependent terms are employed to handle the delayed states $\bar{x}_i$. Whereas, since the LKF (12) is established based on the reconstructed model (6) whose delay-related information is contained in $\bar{x}_{i1}$, the augmented term and H_i and W_i-dependent terms just need to deal with the delayed states $\bar{x}_{i1}$. The following section will verify that the replacement of $\bar{x}_i$ by $\bar{x}_{i1}$ introduces minor conservatism into deriving the delay-dependent stability condition. Moreover, when comparing inequalities (11) and (13), we find that both $\zeta_i(t)$ and $\xi_i(t)$ include the delayed states related information while the latter has a lower dimension. That is, the order of matrix Θ_i is far less than Π_i, which greatly improve the calculation efficiency.

In addition, since Theorem 1.C2 is established through the novel reconstructed model whose gain matrix is separated, it can be extended to design PID controllers with desired dynamic performances based on the methods including the H_∞ theory [21], [22], passivity technique [23], dissipativity [24], [25], exponential stability [26], etc..

B. Exponential stability criterion

The injection of wind power into power system leads to system inertia reduction. To design controllers which have robustness to inertia reduction, [19] proposed delay-dependent state feedback controllers based on the decay rates. When compared with the complex or high-order state feedback controller, the PID-type controller is alternative in industry. Hence, the asymptotical stability criterion is extended to the exponential stability criterion, which is capable of designing decay rate-based PID controller for the delayed LFC scheme considering wind power. Base the novel model reconstruction method, the asymptotical stability condition has features of high accuracy and efficiency. Its extension that the exponential stability criterion can be employed to obtain the PID gains with less time while letting their robustness to wind power disturbance, tie line power change and inertia reduction unchanged.

This part investigates the exponential stability condition for the delayed power system considering wind power, which provides the guideline for designing decay rate-based PID controllers considering the influence of time delay. To show the effective of proposed method, Theorem 2.C1 is firstly established based on the original model, while Theorem 2.C2 employs the novel reconstructed model.

For investigating the exponential stability of the delayed power system integrated with wind energy, an index of decay rate α related to settling time can be introduced, i.e., set $z_i(t)=e^{\alpha t}\bar{x}_i(t)$ by following [27]. Then, system (4) is transformed into

$$\dot{z}_i(t)=(\bar{A}_i+\alpha I)z_i(t)+e^{\alpha\tau_i}\bar{B}_iK_i\bar{C}_iz_i(t-\tau_i). \tag{14}$$

For any $\alpha>0$, the asymptotic stability of (14) implies the exponential stability of the original system model (4) [27].

Thus, using the proposed reconstruction technique leads to

$$\begin{cases}\dot{z}_{i1}(t)=A_{i1\alpha}z_{i1}(t)+A_{i2\alpha}z_{i2}(t)\\ \dot{z}_{i2}(t)=A_{i3\alpha}z_{i1}(t)+A_{i4\alpha}z_{i2}(t)+e^{\alpha\tau_i}b_iK_ic_iz_{i1}(t-\tau_i)\end{cases} \tag{15}$$

where $T_1z_i(t)=\begin{bmatrix}z_{i1}\\ z_{i2}\end{bmatrix}$ and $T_1(\bar{A}_i+\alpha I)T_1^{-1}=\begin{bmatrix}A_{i1\alpha} & A_{i2\alpha}\\ A_{i3\alpha} & A_{i4\alpha}\end{bmatrix}$.

Theorem 2. *For given scalars τ_i,α, system (4) is exponentially stable, if one of the following conditions holds*
C1: there exist symmetric $2n\times 2n$ matrix $P_i>0$, symmetric

$n \times n$ matrices $Q_i > 0, R_i > 0$, such that the following inequality holds

$$\hat{\Pi}_i < 0 \tag{16}$$

where

$$\hat{\Pi}_i = \begin{bmatrix} e_1 \\ \tau_i e_3 \end{bmatrix}^T P_i \begin{bmatrix} \hat{e}_s \\ e_1 - e_2 \end{bmatrix} + \begin{bmatrix} \hat{e}_s \\ e_1 - e_2 \end{bmatrix}^T P_i \begin{bmatrix} e_1 \\ \tau_i e_3 \end{bmatrix} + e_1^T Q_i e_1 - e_2^T Q_i e_2 + \tau_i^2 \hat{e}_s^T R_i \hat{e}_s - \begin{bmatrix} e_1 - e_2 \\ e_1 + e_2 - 2e_3 \end{bmatrix}^T \begin{bmatrix} R_i & 0 \\ 0 & 3R_i \end{bmatrix} \begin{bmatrix} e_1 - e_2 \\ e_1 + e_2 - 2e_3 \end{bmatrix}$$

$$\hat{e}_s = (\bar{A}_i + \alpha I) e_1 + e^{\alpha \tau_i} \bar{B}_i K_i \bar{C}_i e_2$$

with e_j defined as Theorem 1.C1.

C2: there exist symmetric $(2n_1 + n_2) \times (2n_1 + n_2)$ matrix $U_i > 0$, symmetric $n_1 \times n_1$ matrices $H_i > 0, W_i > 0$, such that the following inequality holds

$$\hat{\Theta}_i < 0 \tag{17}$$

where

$$\hat{\Theta}_i = \begin{bmatrix} \vartheta_1 \\ \vartheta_0 \\ \tau_i \vartheta_3 \end{bmatrix}^T U_i \begin{bmatrix} \hat{\vartheta}_{\iota i} \\ \hat{\vartheta}_{\kappa i} \\ \vartheta_1 - \vartheta_2 \end{bmatrix} + \begin{bmatrix} \hat{\vartheta}_{\iota i} \\ \hat{\vartheta}_{\kappa i} \\ \vartheta_1 - \vartheta_2 \end{bmatrix}^T U_i \begin{bmatrix} \vartheta_1 \\ \vartheta_0 \\ \tau_i \vartheta_3 \end{bmatrix} + \vartheta_1^T H_i \vartheta_1 - \vartheta_2^T H_i \vartheta_2 + \tau_i^2 \hat{\vartheta}_{\iota i}^T W_i \hat{\vartheta}_{\iota i} - \begin{bmatrix} \vartheta_1 - \vartheta_2 \\ \vartheta_1 + \vartheta_2 - 2\vartheta_3 \end{bmatrix}^T \begin{bmatrix} W_i & 0 \\ 0 & 3W_i \end{bmatrix} \begin{bmatrix} \vartheta_1 - \vartheta_2 \\ \vartheta_1 + \vartheta_2 - 2\vartheta_3 \end{bmatrix}$$

$$\hat{\vartheta}_{\iota i} = A_{i1\alpha} \vartheta_1 + A_{i2\alpha} \vartheta_0$$

$$\hat{\vartheta}_{\kappa i} = A_{i3\alpha} \vartheta_1 + A_{i4\alpha} \vartheta_0 + e^{\alpha \tau_i} b_i K_i c_i \vartheta_2$$

with ϑ_j and ϑ_0 expressed in Theorem 1.C2.

Proof. For system (14), replacing $\bar{A}_i$ and $\bar{B}_i K_i \bar{C}_i$ in Theorem 1.C1 with $(\bar{A}_i + \alpha I)$ and $e^{\alpha \tau_i} \bar{B}_i K_i \bar{C}_i$, respectively, gives (16). For system (15), replacing $A_{i11}, A_{i12}, A_{i21}, A_{i22}$ and $b_i K_i c_i$ that presented in Theorem 1.C2 with $A_{i1\alpha}, A_{i2\alpha}, A_{i3\alpha}, A_{i4\alpha}$ and $e^{\alpha \tau_i} b_i K_i c_i$, respectively, derives (17). Then, following the similar line in [27], we can conclude that the holdings of LMIs in the Theorem 2.C1 and Theorem 2.C2 guarantee the exponential stability of systems (4) and (6), respectively.

C. Summary of presented method

The following steps of how to implement the presented method are given.

Step1. Model establishment. The state-space model of area i in the multi-area LFC system equipped with PID controller is shown in Section II.A Then, a novel method for reconstructing the original system model is presented in Section II.B.

Step2. Stability analysis. The asymptotical stability condition is established for both the original model and the novel reconstructed model. It is extended to the exponential analysis of delayed power system considering wind power. When the upper bound of time delay is given, the allowable maximum decay rate is calculated. For a desired decay rate, the delay margin can be obtained as well.

Step3. Controller design. Based on the reconstructed model and the original model, for a preset delay upper bound, the controller gains are optimized by maximizing the index of decay rate through selecting PSO algorithm.

Step4. Case studies. Case studies are carried out to show the proposed method is effective.

IV. Case studies

The first case study is tested on the two-area traditional LFC scheme. This case aims to demonstrate the novel reconstructed model can be employed to estimate the effects of the time delays on system stability without introducing conservatism. The other two case studies consider the two-area LFC scheme and three-area one with wind power under the traditional and deregulated environment, respectively. Simulation results demonstrate that, the stability criterion derived by using the novel reconstructed model can not only improve the efficiency of obtaining PID controller gains, but also their robustness to inertia reduction, tie-line power change, external disturbances, and time delays is guaranteed.

The simulation studies are carried out based on the Simulink models following the diagram of Fig. 1 and considering some nonlinearities such as generation rate constraints. Firstly, the code written in the m file needs to transfer the essential parameters to the Simulink models by using the *sim* function. Meanwhile, the Simulink models are driven, and the To Workspace module can be employed to transfer the simulation results including the desired system states to the m file, which can be directly called in the m file. Secondly, through the m file, the simulation results are presented with curves and figures by using the *plot* function.

A. Accuracy improvement

The proposed criterion in [13] based on a reconstructed model enables the calculation efficiency to be improved. Since this reconstructed method is presented without considering the special features of delayed LFC scheme, in some cases, we find the calculation accuracy is decreased a lot by using the reconstructed model and analyzing the system stability. The two-area traditional LFC scheme with the PI controller contained is taken as an example. Hence, in order to use the reconstructed model to accurately estimate the effects of time delays on system frequency stability, and to design controllers to eliminate these effects, a novel reconstructed method should be proposed.

Under traditional environment, the two-area LFC systems with different PI controllers ($K_{P1} = 0.4, K_{I1} = 0.2, K_{P2} = 0.4, K_{I2} = 0.3$), the delay margin calculated through Theorem 1 in [13] (τ_{com}), Theorem 1.C1 (τ_{c_1}) and Theorem 1.C2 (τ_{c_2}) in this paper are listed in Table I. Moreover, to further validate the proposed method based on the time domain method can derive results with minor conservatism when compared with the exact method, the real value for delay margins (τ_r) are developed based on the simulation results and they are shown in Table I. In this table, $\tau = \sqrt{\tau_1^2 + \tau_2^2}$ represents magnitude of τ_1 and τ_2 and $\theta = \tan^{-1}(\tau_1/\tau_2)$. Also, the relative error (ρ) is defined with

$$\rho = \frac{|\tau_\nu - \tau_r|}{\tau_r} \times 100\% \tag{18}$$

TABLE I
DELAY MARGINS IN TRADITIONAL TWO-AREA LFC SYSTEM WITH DIFFERENT PI CONTROLLERS

	$K_{P1}=0.4, K_{I1}=0.2$				$K_{P2}=0.4, K_{I2}=0.3$			
θ	$\tau_{com}(\rho)$	$\tau_{c_1}(\rho)$	$\tau_{c_2}(\rho)$	τ_r	$\tau_{com}(\rho)$	$\tau_{c_1}(\rho)$	$\tau_{c_2}(\rho)$	τ_r
0°	7.13(15.4%)	7.53(10.7%)	7.50(11.0%)	8.43	4.86(9.3%)	5.11(4.7%)	5.06(5.6%)	5.36
20°	8.15(9.2%)	8.73(2.8%)	8.65(3.7%)	8.98	5.63(2.4%)	5.76(0.2%)	5.75(0.3%)	5.77
40°	11.10(0.4%)	11.11(0.4%)	11.11(0.4%)	11.15	7.15(0.4%)	7.16(0.3%)	7.16 (0.3%)	7.18
45°	11.84(0.9%)	11.87(0.7%)	11.87(0.7%)	11.95	7.57(0.5%)	7.58(0.4%)	7.58(0.4%)	7.61
50°	10.97(0.6%)	10.97(0.6%)	10.97(0.6%)	11.04	6.98(0.4%)	6.99(0.3%)	6.99(0.3%)	7.01
70°	7.86(12.4%)	8.65(3.6%)	8.57(4.5%)	8.97	5.51(3.5%)	5.64(1.2%)	5.62(1.6%)	5.71
90°	6.98(17.2%)	7.59(10.0%)	7.44(11.7%)	8.43	4.80(10.4%)	5.03(6.2%)	4.97(7.3%)	5.36

where ν can donate τ_{com}, τ_{c_1}, and τ_{c_2}, respectively.

All research works are finished in the same calculation requirements, i.e., a PC with an imbedded Intel i5 CPU, a 8GB RAM and a 64-bit operation system, and the same presets of computation process. The computation time spent on determining delay margins is recorded in Table II

TABLE II
CALCULATION PERFORMANCE OF THEOREM 1 [13] AND THEOREM 1 IN THIS PAPER

Methods	The.1.C1	The. 1[13](ratio)	The.1.C2 (ratio)
CPU time (s)	124	15(12%)	36 (29%)

From Table I, we can see when the LFC system equipped PI controllers $K_{P1}=0.4, K_{I1}=0.2$, neither Theorem 1.C1 nor Theorem 1.C2 can realize accurate computations of delay margins like the exact method considering $\theta \in [0°, 20°, 70°, 90°]$. Moreover, the same conclusion can be obtained for the case that the LFC system controlled by $K_{P1}=0.4, K_{I1}=0.3$ and $\theta \in [0°, 70°, 90°]$. Despite that, they can derive allowable bigger results to approach the real values in comparison with the methods in [13]. When $\theta \in [40°, 45°, 50°]$, the time domain based methods Theorem 1.C1 and Theorem 1.C2 can still realize accurate delay margins. Especially, although Theorem 1.C2 is established based on the reconstructed model, it can obtain the almost same delay margins as Theorem 1.C1 using the original system model. That is, the conservatism introduced by using the reconstructed model is minimized, and the novel reconstruction method proposed in this paper can be applied for delay-dependent stability analysis of delayed LFC schemes without sacrificing computational accuracy.

According to Table II, even though Theorem 1.C2 spends more time on finding delay margin than Theorem 1 in [13], it only takes 29 percent of time consumed by Theorem 1.C1 based on the original model. Thus, there exists a tradeoff between calculation efficiency and accuracy, and it is acceptable.

B. Decay rate-based PID controller design

The time delay of each area is assumed to have same upper bound equal to $3s$. The exponential stability of the system is guaranteed through Theorem 2 which shows the requirements of controller gains. Given delay bound τ_i and controller gain K_i, the maximal value of decay rate α_{max} can be addressed. α_{max} is a function of τ_i and K_i.

$$\alpha_{max} = g(\tau_i, K_i) = g(h, K_{Pi}, K_{Ii}, K_{Di}) \tag{19}$$

For a preset time delay, to provide optimal robust performance for inertia reduction and the disturbance of wind power, the control gains are improved by solving the optimisation problem.

Maximize $\alpha_{max} = g(h, K_{Pi}, K_{Ii}, K_{Di})$

Subject to $K_{Pimin} \le K_{Pi} \le K_{Pimax}$, $K_{Iimin} \le K_{Ii} \le K_{Iimax}$, and $K_{Dimin} \le K_{Di} \le K_{Dimax}$.

This problem can be addressed by various kinds of optimisation algorithms. This paper chooses the PSO algorithm that is widely employed in numerical optimisation thanks to its excellent behaviors [28].

The PSO algorithm is partially initialized with the following parameters. Set position bounds, $X_{min}=-1$ and $X_{min}=1$, velocity bounds $V_{min}=-0.3$ and $V_{min}=0.3$, population size, $N=20$ and the maximal iteration times $k_{max}=30$. The detailed procedure can be found in [28].

Hence, under traditional environment, controller gains K_1 and K_2 can be determined by Theorem 1.C1 and Theorem 1.C2, respectively. Both of them are listed in Table III. When the case study is carried out under the deregulated three-area LFC scheme, similar steps can help obtain controllers K_3 and K_4, and Table IV shows these results. The solutions of K_1 and K_3 based on the original model are presented to make comparisons with K_2 and K_4 in the terms of calculation efficiency and robust performance such that the effectiveness of employing the novel reconstructed model is demonstrated.

TABLE III
CONTROLLERS DETERMINED BY THEOREM 2.C1 (K_1) AND THEOREM 2.C2 (K_2)

area	K_1	α	K_2	α
1	[-0.16 -0.16 -0.12]	0.0592	[-0.13 -0.13 -0.13]	0.0592
2	[-0.18 -0.18 -0.18]	0.0580	[-0.15 -0.15 -0.042]	0.0580

TABLE IV
CONTROLLERS DETERMINED BY THEOREM 2.C1 (K_3) AND THEOREM 2.C2 (K_4)

area	K_3	α	K_4	α
1	[-0.007 -0.15 -0.002]	0.20	[-0.007 -0.118 -0.007]	0.19
2	[-0.066 -0.118 -0.01]	0.31	[-0.076 -0.121 -0.013]	0.31
3	[-0.046 -0.17 0.015]	0.21	[-0.023 -0.123 0.022]	0.20

Theorem 2.C1 and Theorem 2.C2 are both used to calculate the gains of PID controller through PSO algorithm. Table V records the time consumed, where notations t_{c_1} and t_{c_2} represent the time in seconds required by Theorem 2.C1 and Theorem 2.C2, respectively. From Table V, when the

traditional two-area LFC scheme is considered with one generator in each area, the time consumed by Theorem 2.C2 just accounts for around 50 percent of that used by Theorem 2.C1. That is, Theorem 2.C2 based on the reconstructed model is able to improve the calculation efficiency for PID controller. Considering the three-area LFC scheme under deregulated environment and each area is assumed to have two Gencos and two Discos, we can find that it will take Theorem 2.C1 more than three times of time that spent by Theorem 2.C2. It can be concluded that more generators (Gencos) are included in one area, more time will be required to obtain PID gains. In this two cases, although the order of system model is just increased by 2, the time consumption behaves a sharp rise. Therefore, it is essential to apply the novel reconstructed model to establishing stability criterion such that less time will be demanded to obtain PID gains, especially if more generators (Gencos) are included in one area.

TABLE V
COMPARISON OF COMPUTATION PERFORMANCE BETWEEN THEOREM 2.C1 AND THEOREM 2.C2

	Traditional			Deregulated		
	K_1	K_2	Ratio(%)	K_3	K_4	Ratio(%)
area	$t_{c_1}(s)$	$t_{c_2}(s)$	t_{c_2}/t_{c_1}	$t_{c_1}(s)$	$t_{c_2}(s)$	t_{c_2}/t_{c_1}
1	761	385	51%	3325	1139	34%
2	715	373	52 %	4647	1666	36%
3	-	-	-	1049	3145	33%

C. Simulation verification

In order to show the controllers obtained form the reconstructed model performance as well as that derived from original model, two simulation cases are considered including the two-area traditional LFC scheme and three-area deregulated one. Both of them are integrated with wind power. Each case has designed three scenarios.

Firstly, each area are assumed to have one generator in the traditional LFC scheme. For scenario 1 (S_1), there appears a step change with 0.1 pu from wind power in each area. After 5 seconds, a step load demand with 0.2 pu is introduced into two areas. The area control error (ACE) of the first area regulated by controller K_1 is drawn with blue dotted line in Fig. 2, where the performance of K_2 is recorded with the red solid line. Fig. 2 (a) shows the curves of ACE considering zero inertia reduction in the LFC scheme. When there exists 30% inertia reduction, Fig. 2 (b) shows how the ACE changes with the introduction of wind power and load disturbance. Similarly, in the following scenarios, Fig. (a) is based on the normal LFC schemes while Fig. (b) is obtained under the system with 30% inertia reduction.

For scenario 2 (S_2), the random change of wind power with the amplitude of 0.1 pu is assumed for each area at $t = 0$. A step load disturbance having 0.2 pu amplitude is added to each area at $t = 5$. Then, the ACEs of LFC schemes equipped controllers K_1 or K_2 are shown in Fig. 3.

For scenario 3 (S_3), the controllers K_1 and K_2 are designed under constant time delay $\tau_i = 3s$. This test is to check whether they have similar robustness against time delays considering (a) $\tau_i = 5s$ or (b) $\tau_i \in [2, 8]s$. Here, we still

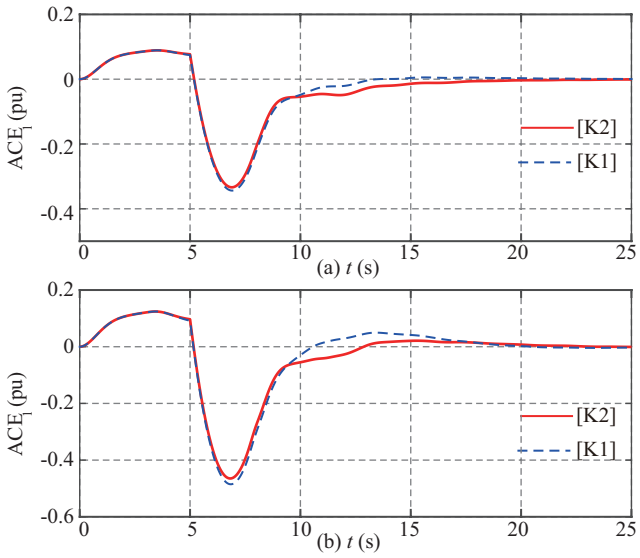

Fig. 2. The ACE of area 1 in the traditional two-area LFC scheme with inertia reductions (a) 0%; (b) 30%.

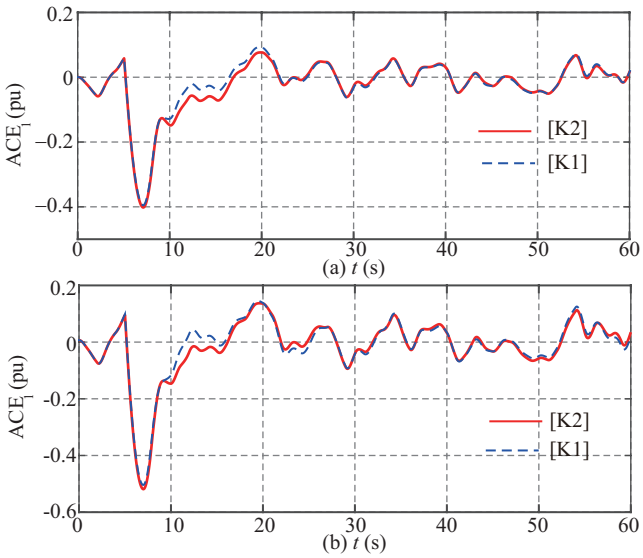

Fig. 3. The ACE of area 1 in the traditional two-area LFC scheme with inertia reductions (a) 0%; (b) 30%.

assume the same types of wind power and load change as scenario 2 are introduced into the traditional two-area LFC scheme. The system response for area 1 is shown in Fig. 4 with time delay $\tau_i = 5s$. The random time delay $\tau_i \in [2, 8]s$ is depicted in the first picture of Fig. 5 where the ACE_1 of the two-area LFC scheme is also described accordingly.

Secondly, for deregulated case, each area contains two Gencos and Discos. The constraint of generator rate is assumed to be ± 0.1 pu/min. The AGPM is listed to show the contract for the Discos and the Gencos as follow.

$$AGPM = \begin{bmatrix} 0.25 & 0 & 0.25 & 0 & 0.5 & 0 \\ 0.5 & 0.25 & 0 & 0.25 & 0 & 0 \\ 0 & 0.5 & 0.25 & 0 & 0 & 0 \\ 0.25 & 0 & 0.5 & 0.75 & 0 & 0 \\ 0 & 0.25 & 0 & 0 & 0.5 & 0 \\ 0 & 0 & 0 & 0 & 0 & 1 \end{bmatrix}. \quad (20)$$

The load disturbance with 0.1 pu step change appears in

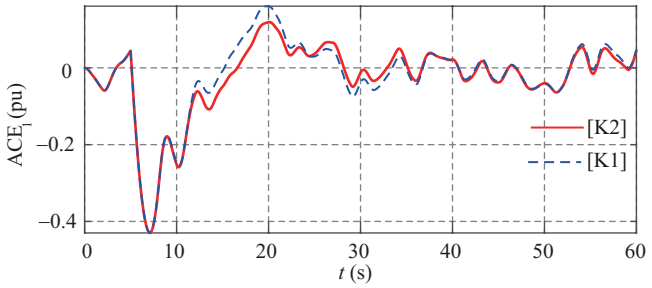

Fig. 4. The ACE of area 1 in the traditional two-area LFC scheme with constant delays ($\tau_i = 5s$)

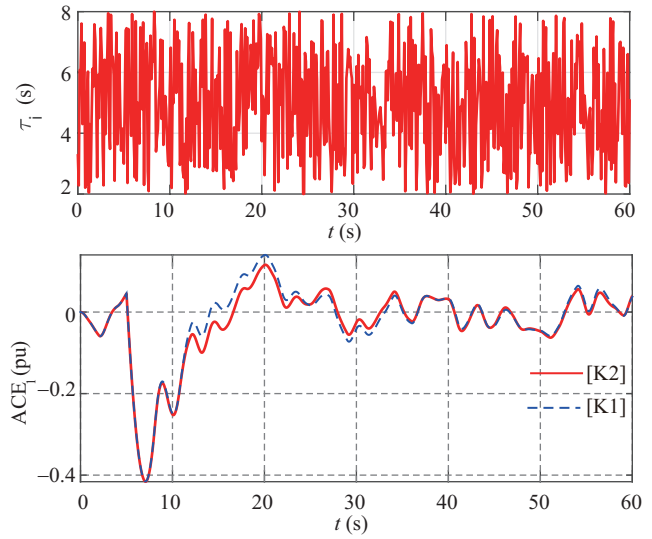

Fig. 5. The ACE of area 1 in the traditional two-area LFC scheme with random delays ($\tau_i \in [2, 8]s$)

each Disco ($\Delta P_{Li} = 0.2$pu), and Disco 1 in area 1 and 2 as well as Disco 2 in area 3 demands 0.05pu, 0.04pu and 0.03pu as un-contracted loads ($\Delta P_{\mathrm{d}1} = 0.05\mathrm{pu}, \Delta P_{\mathrm{d}2} = 0.04\mathrm{pu}, \Delta P_{\mathrm{d}3} = 0.03\mathrm{pu}$).

For scenario 4 (S_4), at $t = 0$, a step change of 0.15 pu for wind power is introduced. Two curves in Fig. 6 display the variation tendencies of the ACEs in area 1 equipped with K_3 and K_4, respectively.

For scenario 5 (S_5), when the disturbance of wind power is a random change with 0.1 pu, Fig. 7 shows, in area 1, how the ACEs controlled by K_3 and K_4 change.

For scenario 6 (S_6), two kinds of time delays are assumed to be introduced into the deregulated three-area LFC scheme, i.e., (a) constant time delays $\tau_i = 8s$, (b) random time delays $\tau_i \in [2, 10]s$. Meanwhile, the random wind power and load disturbance are added to the related system, whose values are given in scenario 5. This scenario is designed to demonstrate controller K_4 which is based on the reconstructed model behaves the same robustness to time delays as controller K_3 does, as both of them are designed with the consideration of $\tau_i = 3s$. Therefore, Fig.8 shows the ACEs of area 1 controlled by K_3 or K_4. The random delays are expressed in Fig.9 In this figure, the system responses of area 1 are also recorded when the random delays are introduced into the transmission

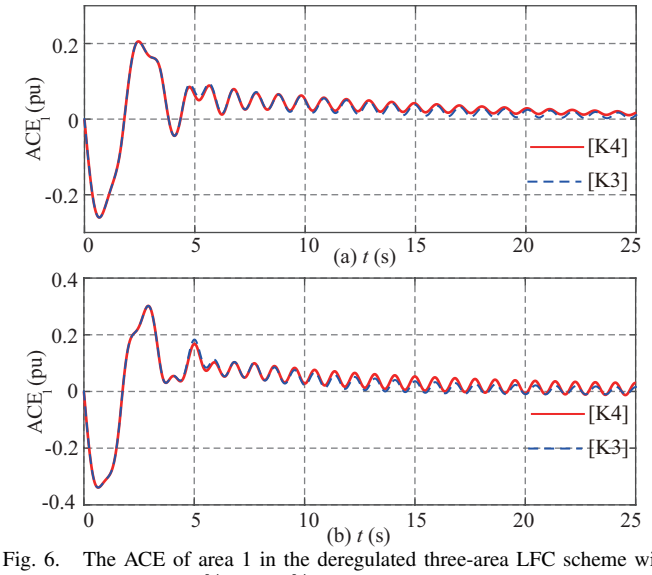

Fig. 6. The ACE of area 1 in the deregulated three-area LFC scheme with inertia reductions (a) 0%; (b) 30%.

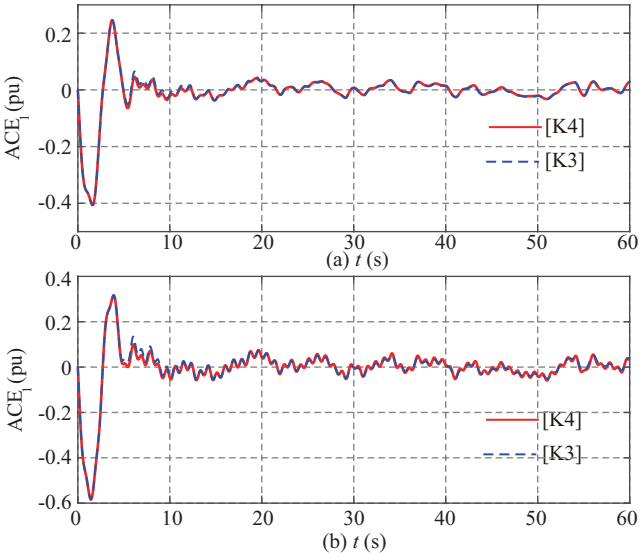

Fig. 7. The ACE of area 1 in the deregulated three-area LFC scheme with inertia reductions (a) 0%; (b) 30%.

channels of the deregulated three-area LFC system.

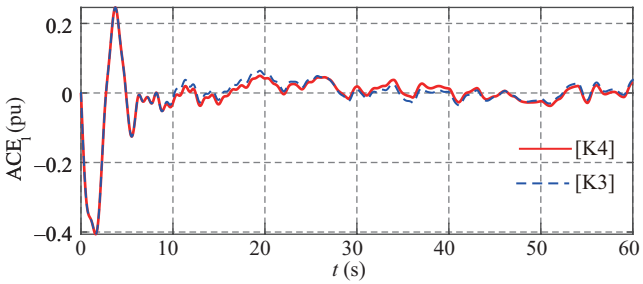

Fig. 8. The ACE of area 1 in the deregulated two-area LFC scheme with constant delays ($\tau_i = 8s$)

The integral of the time multiplied absolute value of the error (ITAE) is defined as

$$ITAE = \int_0^{t_{end}} t(|ACE_1|)dt \tag{21}$$

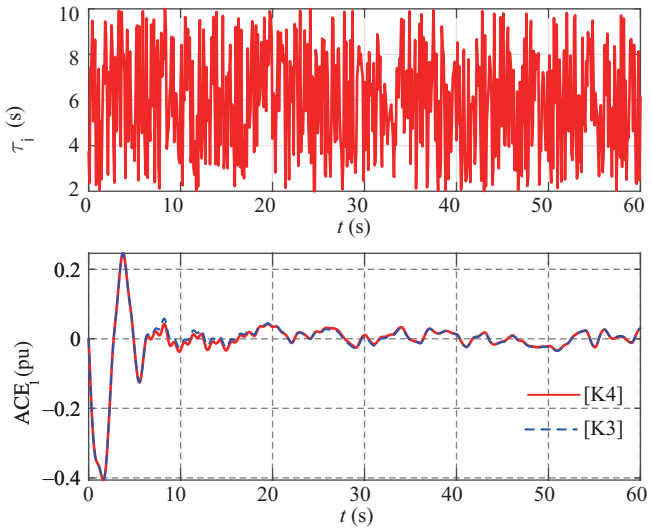

Fig. 9. The ACE of area 1 in the deregulated three-area LFC scheme with random delays ($\tau_i \in [2, 10]s$)

where t_{end} is equal to the simulation time.

The ITAEs are calculated for above six scenarios and they are listed in Table VI.

TABLE VI
PERFORMANCE INDICES OF ITAE FOR DIFFERENT SCENARIOS

ITAE (Traditional)			ITAE (Deregulated)		
Scenarios	K_1	K_2	Scenarios	K_3	K_4
S_1(a)	9.08	10.42	S_4(a)	7.95	9.52
S_1(b)	14.66	13.13	S_4(b)	8.52	10.65
S_2(a)	58.80	58.78	S_5(a)	28.66	28.22
S_2(b)	83.25	84.24	S_5(b)	42.68	42.84
S_3(a)	72.92	77.50	S_6(a)	32.09	32.90
S_3(b)	62.44	65.49	S_6(b)	29.05	29.24

As can be seen from Fig.2, both controllers K_1 and K_2 can eliminate the ACE within $20s$ after a step change is introduced into the traditional LFC scheme. When there is 30% inertial reduction, K_1 and K_2 still enable the ACE to be zero. Hence, the robustness of K_1 and K_2 to inertial reduction can be verified. For scenario 2, the random wind power is added to the traditional two-area power system. Fig.3 confirms that the almost identified robustness against disturbance of wind power belongs to K_1 and K_2 regardless of the inertia being reduced from 0% to 30%. From Fig.4, although both controllers K_1 and K_2 are designed considering $\tau_i = 3s$, their dynamic performances are not changed obviously when the tested time delay is given as $5s$. Moreover, controller K_2 still behaves as well as K_1. Additionally, if the random time delay shown as Fig.5 are taken into account, same conclusion can be obtained as the constant time delays introduced into the LFC system. Therefore, the extremely similar robustness against time delays is verified between controllers K_1 and K_2.

Based on Fig.6 and Fig.7, controllers K_3 and K_4 which are calculated using standard parameters are verified to have robustness against system parameter variations. When different kinds of time delays are assumed in the simulations, Fig.8 and Fig.9 validate both controllers K_3 and K_4 are tolerated to time delays. In these two figures, the similar tendency of curves further shows the reconstructed model proposed in this paper can be used to develop controllers without reducing their dynamic performance.

In Table VI, the ITAEs numerically show that, under traditional environment, there only exists a little difference between controller K_1 and K_2. For the deregulated case, similar conclusion can be obtained for controllers K_3 and K_4.

V. Conclusion

This paper has proposed a novel method to reconstruct the system model for the power system with wind energy and time delay. This novel method has been formed by taking the special features of delayed LFC system into account, based on which the conservatism contained in the asymptotical stability criterion has been minimized. More importantly, this reconstructed method is available for deriving controller gains. The established asymptotical stability criterion has been extended to the exponential stability condition, which is able to guide the design of decay rate-based PID controller for the delayed LFC scheme with wind power. Based on the criteria using the novel reconstructed model, the efficiency of obtaining controller gains has been apparently improved while guaranteeing their robustness to wind disturbance, tie line power change and inertia reduction when compared with the controllers based on the original model.

Case study has been completed using the traditional two-area power system to validate the merit of reconstructed model in enhancing the calculation accuracy. Then, in order to demonstrate the novel reconstructed model can be used to establish criterion and to design controller gains with high efficiency while keeping their dynamic performance, case studies are tested on the two-area and three-area LFC schemes under traditional and deregulated environments, respectively. The developed controller based on the novel reconstructed model has been verified to performance as well as the controller resorting the model before reconstruction.

Since the power systems become increasingly interconnected, the wide-area damping control systems (WADCs) using remote feedback signals is an alternative method to address the low-frequency inter-area oscillation. The WADCs utilize remote signals as inputs, which relies on the communication networks to transmit the signals and therefore, the feedback signals of wide-area controllers are also time-delayed inevitably. This scenario is similar to the LFC system with communication delays. As a result, the presented approach based on the delayed LFC scheme can be extended to the delay-dependent stability analysis of WADCs involving time delays with improved computation efficiency. Moreover, it is also applicable that the proposed approach is used to determine the controller gains of WADCs with less time consumption while guaranteeing their dynamic performances unchanged obviously.

Appendix I

The parameters that are required in the traditional two-area LFC scheme with each area containing one generator, are listed in Table VII. Also, the deregulated three-area LFC scheme is parameterized in Table VIII where one area contains two Gencos and Discos.

TABLE VII
TRADITIONAL TWO-AREA LFC SYSTEM AND EACH AREA INCLUDING ONE GENERATOR

Parameters	T_t	T_g	R	D	β	M	α	T_{12}
Area1	0.30	0.10	0.05	1.00	21.0	10	1.00	0.1968
Area2	0.40	0.17	0.05	1.50	21.5	12	1.00	

TABLE VIII
DEREGULATED THREE-AREA LFC SCHEME AND EACH AREA INCLUDING TWO GENCOS AND DISCOS

Parameters	($k-i$: k in area i)							Areas		
	1-1	2-1	1-2	2-2	1-3	2-3		1	2	3
T_t	0.32	0.30	0.30	0.32	0.31	0.34	M	0.1667	0.2084	0.1600
T_g	0.06	0.08	0.06	0.07	0.08	0.06	D	0.0084	0.0084	0.0080
R	2.4	2.5	2.5	2.7	2.8	2.4	β	0.4250	0.3966	0.3522
α	0.5	0.5	0.5	0.5	0.6	0.4	T_{ij}	T_{12}=0.2450	T_{13}=0.212	T_{23}=0

REFERENCES

[1] E.G. Tian, C. Peng, "Memory-based event-triggering H_∞ load frequency control for power systems under deception attacks," *IEEE Trans. Cybern.,* DOI: 10.1109/TCYB.2020.2972384, 2020.

[2] L. Jiang, W. Yao, Q.H. Wu, et al. "Delay-dependent stability for load frequency control with constant and time-varying delays," *IEEE Trans. Power Syst.,* vol. 27, no. 2, pp. 932-941, 2012.

[3] X.C. Shangguan, Y. He, C.K. Zhang, et al. "Robust load frequency control for power system considering transmission delay and sampling period," *IEEE Trans. Industr. Inform.,* DOI: 10.1109/TII.2020.3026336, 2021.

[4] C. Deng, C.Y. Wen, "MAS-based distributed resilient control for a class of cyber-physical systems with communication delays under DoS attacks," *IEEE Trans. Cybern.,* DOI:10.1109/TCYB.2020.2972686, 2020.

[5] X. Peng, W. Yao, C. Yan, et al. "Two-stage variable proportion coefficient based frequency support of grid-connected DFIG-WTs," *IEEE Trans. Power Syst.,* vol. 35, no. 2, pp. 962-974, 2019.

[6] K. Dehghanpour, S. Afsharnia, "Electrical demand side contribution to frequency control in power systems: a review on technical aspects," *Renewable Sustainable Energy Rev.,* vol. 41, pp. 1267-76, 2015.

[7] N. Nguyen, J. Mitra, "An analysis of the effects and dependency of wind power penetration on system frequency regulation," *IEEE Trans. Sustainable Energy,* vol. 7, no. 1, pp. 354-363, 2016.

[8] J. Chen, S. Meng, J. Sun, "Stability analysis of networked control systems with aperiodic sampling and time-varying delay," *IEEE Trans. Cybern.,* vol. 47, no. 8, pp. 2312-2320, 2017.

[9] F. Yang, J. He, Q. Pan, "Further improvement on delay-dependent load frequency control of power systems via truncated B-L inequality," *IEEE Trans. Power Syst.,* vol. 33, no. 3, pp. 5062-5071, 2018.

[10] F. Yang, J. He, D. Wang, "New stability criteria of delayed load frequency control systems via infinite-series-based inequality," *IEEE Trans. Industr. Inform.,* vol. 14, no. 1, pp. 231-240, 2018.

[11] C. Duan, C.K. Zhang, L. Jiang, et al. "Structure-exploiting delay-dependent stability analysis applied to power system load frequency control," *IEEE Trans. Power Syst.,*, vol. 32, no. 6, pp. 4528-4540, 2017.

[12] X.D. Yu, H.J. Jia, C.S. Wang, "CTDAE and CTODE models and their applications to power system stability analysis with time delays," *Sci. China Tech. Sci.,* vol. 56, no. 5, pp. 1213-1223, 2013.

[13] L. Jin, C.K. Zhang, Y. He, et al. "Delay-dependent stability analysis of multi-area load frequency control with enhanced accuracy and computation efficiency," *IEEE Trans. Power Syst.,* vol. 34, no. 5, pp. 3687-3696, 2019.

[14] C.K. Zhang, L. Jiang, Q.H. Wu, et al. "Delay-dependent robust load frequency control for time delay power systems," *IEEE Trans. Power Syst.,* vol. 28, no. 3, pp. 2192-2201, 2013.

[15] C. Peng, J. Zhang, "Delay-distribution-dependent load frequency control of power systems with probabilistic interval delays," *IEEE Trans. Power Syst.,* vol. 31, no. 4, pp. 3309-3317, 2016.

[16] J.F. Dai, Y. Tang, Q. Wang, "Fast method to estimate Maximum penetration level of wind power considering frequency cumulative effect" *IET Gener. Transm. Distrib.,* vol. 13, no. 9, pp. 1726-1733, 2019.

[17] Z. Afshar, N.T. Bazargani, S.M.T. Bathaee, "Virtual synchronous generator for frequency response improving and power damping in microgrids using adaptive sliding mode control," *Proceedings of the 10th International Conference and Exposition on Electrical and Power Engineering*, pp. 199-204, 2018.

[18] M. Chilali, P. Gahinet, "H_∞ design with pole placement constraints: an LMI approach," *IEEE Trans. Automat. Contr.,* vol. 41, no. 3, pp. 358-367, 1996.

[19] X.C. Shangguan, Y. He, C.K. Zhang, et al. "Sampled-data based discrete and fast load frequency control for power systems with wind power," *Appl. Energy*, 114202, 2020.

[20] M. Wu, Y. He, J.H. She, *"Stability analysis and robust control of time-delay systems,"* New York: Springer, 2010.

[21] C. Peng, J. Li, M. Fei, "Resilient event-triggering H_∞ load frequency control for multi-area power systems with energy-limited DoS attacks," *IEEE Trans. Power Syst.,* vol. 32. no. 5, pp. 4110-4118, 2017.

[22] C. Peng, J. Zhang, H. Yan, "Adaptive event-triggering H_∞ load frequency control for network-based power systems," *IEEE Trans. Ind. Electron.,* vol. 65, no. 2, pp. 1685-1694, 2018.

[23] H. Huerta, A.G. Loukianov, J.M. Canedo, "Passivity sliding mode control of large-scale power systems," *IEEE Trans. Control Syst. Technol.,* vol. 27, no. 3, pp. 1219 - 1227, 2018.

[24] L. Jin, Y. He, L. Jiang, et al. "Extended dissipativity analysis for discrete-time delayed neural networks based on an extended reciprocally convex matrix inequality," *Inf. Sci.,* vol. 462, pp. 357-366, 2018.

[25] R.J Ma, P. Shi, L.G. Wu, Dissipativity-based sliding-mode control of cyber-physical systems under denial-of-service attacks," *IEEE Trans. Cybern.,* DOI: 10.1109/TCYB.2020.2975089, 2020.

[26] Y. He, M.D. Ji, C.K. Zhang, et al. "Global exponential stability of neural networks with time-varying delay based on free-matrix-based integral inequality," *Neural Netw.,* vol. 77, pp. 80-86, 2016.

[27] K. Liu, E. Fridman, "Wirtinger's inequality and Lyapunov-based sampled-data stabilization," *Automatica*, vol. 48, pp. 102-108, 2012.

[28] H. Fan, L. Jiang, C.K. Zhang, et al. "Frequency regulation of multi-area power systems with plug-in electric vehicles considering communication delays," *IET Gener. Transm. Distrib.,* vol. 10, no. 14, pp. 3481-3491, 2016.

Li Jin (S-19) received the B.S. degree in automation from China University of Geosciences, Wuhan, China, in 2016 and is pursuing the Ph.D. degree in control science and engineering from China University of Geosciences.

She was a joint Ph.D. student with the Department of Electrical Engineering and Electronics, University of Liverpool, Liverpool, U.K., from 2018 to 2020. Her current research interests include time-delay systems, robust control, power system stability analysis and control.

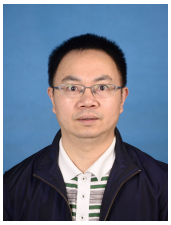

Yong He (SM-06) received the B.S. and M.S. degrees in applied mathematics and the Ph.D. degree in control theory and control engineering from Central South University, Changsha, China, in 1991, 1994, and 2004, respectively.

He was a Lecturer with the School of Mathematics and Statistics, Central South University, and later a Professor with the School of Information Science and Engineering, Central South University, from 1994 to 2014. He was a Research Fellow with the Department of Electrical and Computer Engineering, National University of Singapore, Singapore, from 2005 to 2006, and the Faculty of Advanced Technology, University of Glamorgan, Glamorgan, U.K., from 2006 to 2007. He joined the China University of Geosciences, Wuhan, China, in 2014, where he is currently a Professor with the School of Automation. His current research interests include time-delay systems and networked control systems.

Chuan-Ke Zhang (SM-19) received the B.S. degree in automation and the Ph.D. degree in control science and engineering from Central South University, Changsha, China, in 2007 and 2013, respectively.

He was a Research Associate with the Department of Electrical Engineering and Electronics, University of Liverpool, Liverpool, U.K., from 2014 to 2016. He is currently a Professor with the School of Automation, China University of Geosciences, Wuhan, China. His current research interests include time-delay systems and power systems.

Xing-Chen Shangguan (S-19) received the B.S. degree in automation from China University of Geosciences, Wuhan, China, in 2016 and is pursuing the Ph.D. degree in control science and engineering from China University of Geosciences.

He was a joint Ph.D. student with the Department of Electrical Engineering and Electronics, University of Liverpool, Liverpool, U.K., from 2018 to 2020. His current research interests include sampled-data systems, time-delay systems and power systems.

Lin Jiang (M-00) received his B.S. and M.S. degrees in Electrical Engineering from the Huazhong University of Science and Technology, Wuhan, China, in 1992 and 1996, respectively; and his Ph.D. degree in Electrical Engineering from the University of Liverpool, Liverpool, ENG, UK, in 2001.

He is presently working as a Reader of Electrical Engineering at the University of Liverpool. His current research interests include the optimization and control of smart grids, electrical machines, power electronics and renewable energy.

Min Wu (SM-08/F-19) received the B.S. and M.S. degrees in engineering from Central South University, Changsha, China, in 1983 and 1986, respectively, and the Ph.D. degree in engineering from the Tokyo Institute of Technology, Tokyo, Japan, in 1999.

He was a faculty member of the School of Information Science and Engineering at Central South University from 1986 to 2014, and was promoted to Professor in 1994. In 2014, he joined China University of Geosciences, Wuhan, China, where he is a professor in the School of Automation. He was a visiting scholar with the Department of Electrical Engineering, Tohoku University, Sendai, Japan, from 1989 to 1990, and a visiting research scholar with the Department of Control and Systems Engineering, Tokyo Institute of Technology, from 1996 to 1999. He was a visiting professor at the School of Mechanical, Materials, Manufacturing Engineering and Management, University of Nottingham, Nottingham, U.K., from 2001 to 2002. His current research interests include process control, robust control, and intelligent systems.

Dr. Wu is a Fellow of the IEEE and a Fellow of the Chinese Association of Automation. He received the IFAC Control Engineering Practice Prize Paper Award in 1999 (together with M. Nakano and J. She).